Supporting Information

Wibowo et al. 10.1073/pnas.1308827110

SI Materials and Methods

Purification of Human Folate Receptor α Secreted from *Sf9* Cells. All data presented in the main text result from human folate receptors (hFRs) expressed and purified from Chinese Hamster Ovary (CHO) cells. In the initial stages of this work, two additional hFRα structures at acidic pH were determined with protein produced via standard techniques using a *Spodoptera frugiperda* insect cell (*Sf9*) baculovirus expression system. The first structure was determined using a construct design from which expressed protein contained no fusion tags and encoded hFRα lacking the C-terminal signal peptide that directs glycosyl-phosphatidylinositol (GPI) anchor attachment (hFRα residues 25–234). This protein was purified via folate affinity and size exclusion chromatography as described for hFRs from CHO cells and only protein from a single preparation crystallized in space group $P6_5$ at pH 5.5 (Table S1). Subsequent purifications and crystallization trials never yielded crystals. A second baculovirus was generated that encoded hFRα with its N-terminal signal peptide replaced by that of the honey bee melittin protein. Additionally, the C-terminal GPI anchor sequence was replaced with a hexhistidine affinity tag. hFRα-His_6 was purified via Ni-nitrilotriacetic acid–immobilized metal affinity, folate affinity, and size exclusion chromatography. hFRα purified using this construct crystallized, albeit not reproducibly, in space group P1 (Table S1).

***N*-Glycan Variants of hFRs in Crystallization Trials.** Crystallization trials were conducted for both hFRα and hFRβ purified from CHO cells with three distinct *N*-glycosylation variants at each site of glycan attachment: heterogeneous glycans, homogeneous $Man_9GlcNAc_2$-Asn, and homogeneous GlcNAc-Asn. When cells were cultured in standard growth medium, hFRs possessed a heterogeneous population of glycan structures at each *N*-glycan site owing to addition of monosaccharide units of varying identity in the late stages of maturation (e.g., galactose, *N*-acetyl galactose, sialic acid). To obtain homogeneous $Man_9GlcNAc_2$ *N*-glycans, cells were grown in medium containing 1 mg/L kifunensine (Kif), a potent inhibitor of Golgi α-mannosidase I (1, 2). The resulting high mannose structures are sensitive to processing by endoglycosidase H (EndoH), which cleaves between the first and second GlcNAc (1, 2). After EndoH processing, hFRs possessed a single GlcNAc at each *N*-glycan site. During crystallization trials, hundreds of unique conditions readily yielded needle- or rod-shaped crystals for both apo-hFRα and hFRα–ligand complexes with either heterogeneous or homogeneous Kif *N*-glycans. Unfortunately, none of these crystals gave rise to diffraction with Bragg spacings better than 20 Å. The apo-hFRα Kif-EndoH variant also crystallized at pH values from 4.5 to 6.0, and these crystals gave rise to the highest quality structure of the four models presented herein for apo-hFRα at acidic pH (designated Kif-EndoH in Table S1). Crystals of apo-hFRβ and hFRβ in complex with folate and antifolates were obtained with samples containing heterogeneous *N*-glycans and the high mannose glycans that result from cells grown in the presence of Kif. However, all structures of hFRβ were determined using crystals of hFRβ with heterogeneous *N*-glycans.

1. Elbein AD, Tropea JE, Mitchell M, Kaushal GP (1990) Kifunensine, a potent inhibitor of the glycoprotein processing mannosidase I. *J Biol Chem* 265(26):15599–15605.

2. Kaushal GP, Pastuszak I, Hatanaka K, Elbein AD (1990) Purification to homogeneity and properties of glucosidase II from mung bean seedlings and suspension-cultured soybean cells. *J Biol Chem* 265(27):16271–16279.

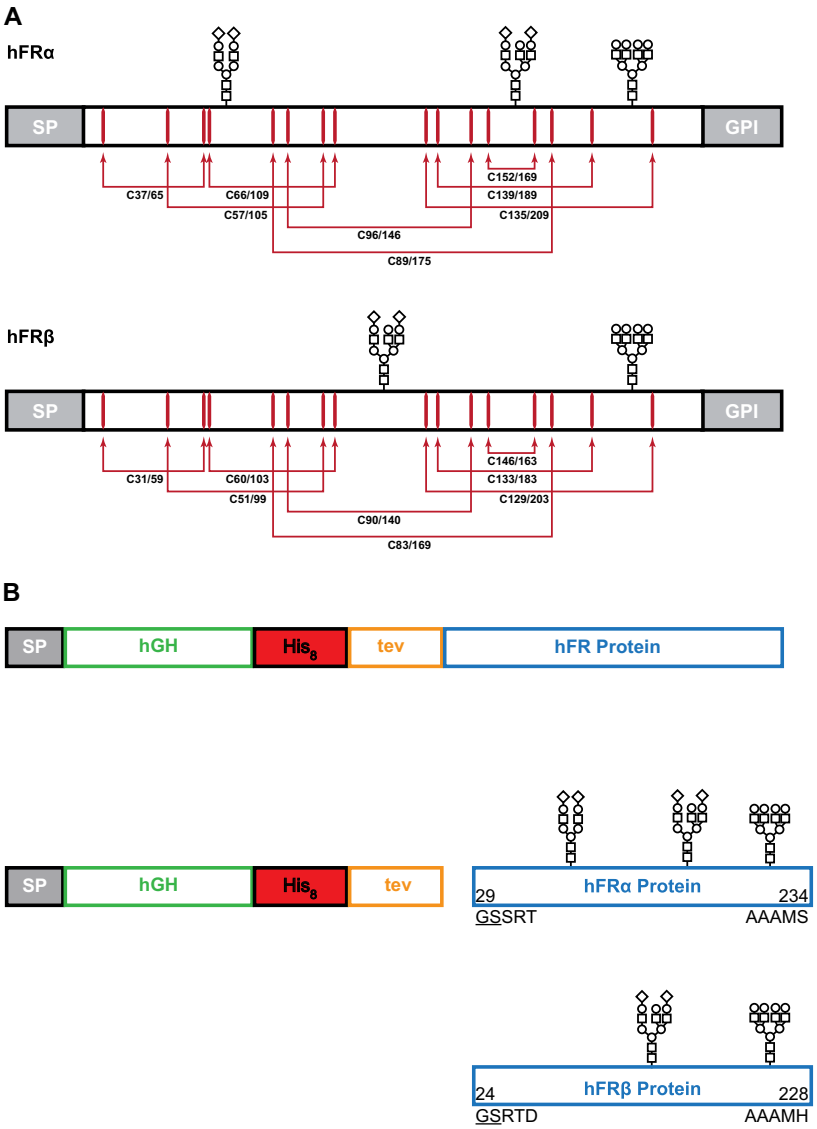

Fig. S1. hFR protein mammalian expression constructs. (*A*) hFRα/β proteins contain N- and C-terminal signal peptides that target the proteins to the secretory pathway (SP) and direct GPI-anchor attachment (GPI), respectively. Both signal sequences are cleaved in the secretory pathway before display of the receptors on the cell surface. The relative positions of heterogeneous *N*-linked glycans are represented, and symbols do not explicitly imply the type of carbohydrate attached. Three *N*-linked glycan sites are present on hFRα (N69, N161, and N201) and two are present on hFRβ (N115 and N195). Only the last glycan site is conserved among the proteins. Additionally, structural analysis has elucidated the specific disulfide bonds formed between the 16 conserved cysteine residues. Pairs are indicated by arrowhead lines. (*B*) The pSGHV0 vector design is presented in Leahy et al. (1). The resultant protein cloned into the pSGHV0 vector encompasses the mature hFR as a C-terminal fusion to human growth hormone (hGH), octahistidine tag (His_8), and a tobacco etch virus protease cleavage site (tev). As the construct includes sequences encoding the native hGH signal peptide, these proteins are secreted when expressed in CHO cells. Residues at the termini of purified hFRα and hFRβ are indicated with sequences resulting from the expression vector underlined.

1. Leahy DJ, Dann CE, III, Longo P, Perman B, Ramyar KX (2000) A mammalian expression vector for expression and purification of secreted proteins for structural studies. *Prot Expr Purif* 20(3):500–506.

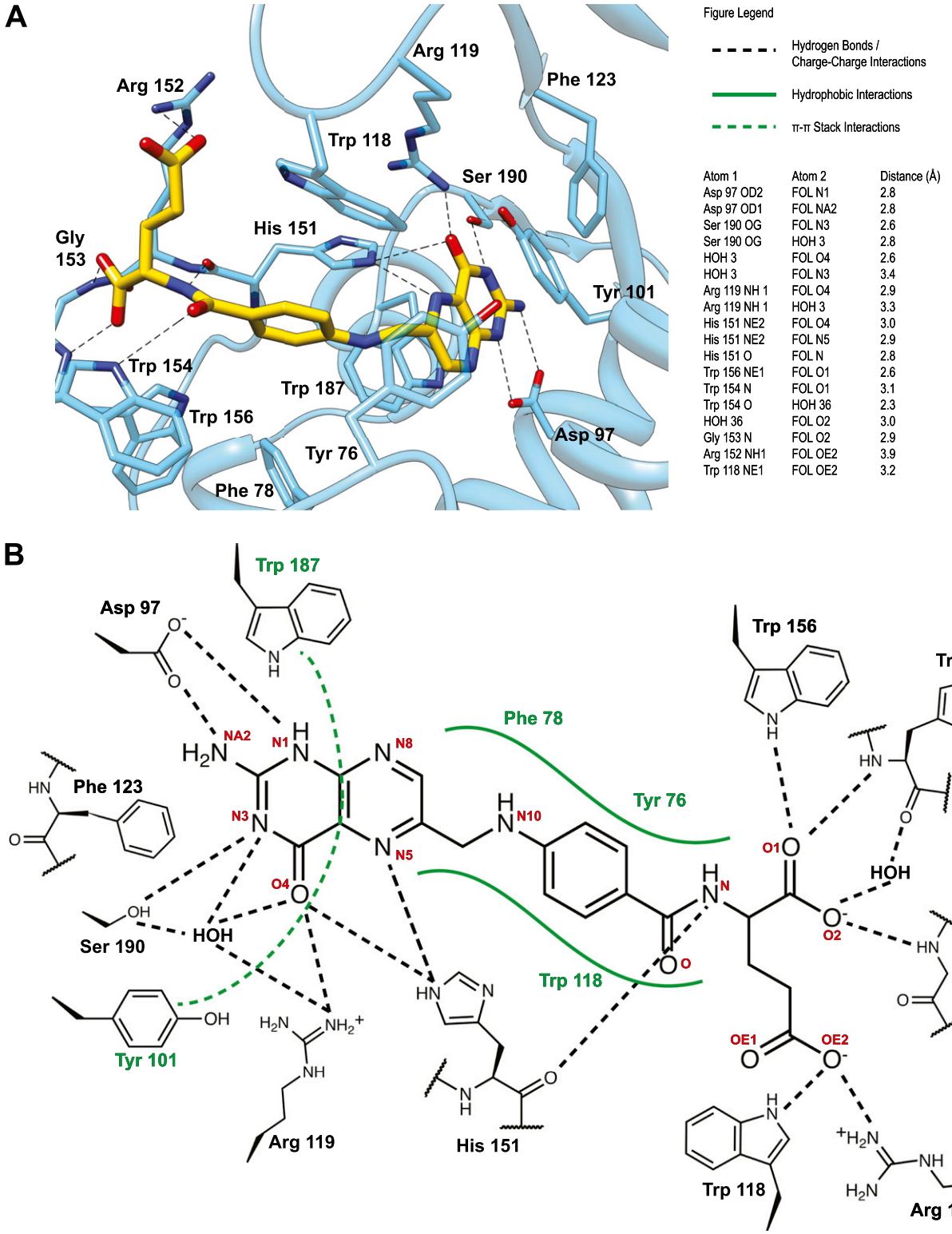

Fig. S2. Ligand interaction map of the hFRβ folate (FOL) complex structure. (*A*) The cartoon image highlights residues in the binding pocket that make direct contact with folate. (*B*) The ligand map shows a schematic of interacting residues. Contact types are listed in the legend in the upper right. Distances between atoms in polar contacts are listed in the table inset. The relative orientation of residues in the interaction maps of Figs. S2 and S4–S6 are fixed to facilitate comparative analysis of similarities and differences in ligand binding among hFR complexes.

RMSD pair	Overall (Å)	Excluding basic loop* (Å)
P1 mol A : P1 mol B	0.157	NA
$P2_12_12_1$: P1 mol A	0.400	NA
$P2_12_12_1$: P1 mol B	0.383	NA
$P2_12_12_1$: $P6_5$	1.159	0.621
P1 mol A : $P6_5$	0.863	0.649
P1 mol B : $P6_5$	0.822	0.606

*The basic loop of the $P6_5$ model was excluded (see legend).

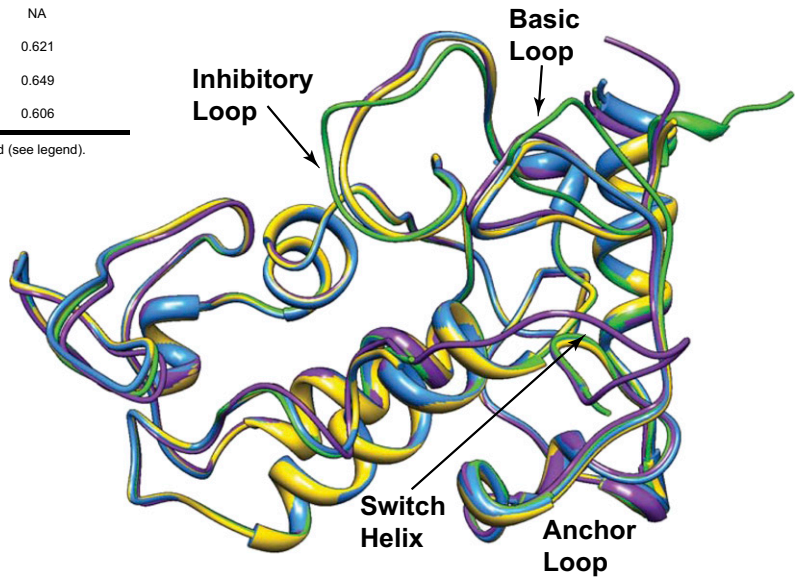

Fig. S3. Superposition of apo-hFRα models. Apo-hFRα from either CHO or *Sf9* cells was crystallized at pH 5.5 in three space groups: $P2_12_12_11$, $P6_5$, and P1 (Table S1). As the P1 crystal formed with two molecules in the asymmetric unit, a total of four apo-FRα models at acidic pH can be compared. The apo-hFRα model from the $P2_12_12_1$ space group, which includes an ordered loop conformation for the switch region, was used for all state III figures in the main text and is colored purple. Molecule A of the P1 model is colored blue, molecule B is colored yellow, and the $P6_5$ model is colored green. The only significant differences in these four structures lies in the basic loop, which has an altered conformation in the $P6_5$ model due to interactions with the N-terminal tryptophan (W28) of a symmetry molecule. Pairwise Cα root mean square deviation calculations for all models including or excluding the basic loop of the $P6_5$ model are included in the figure inset.

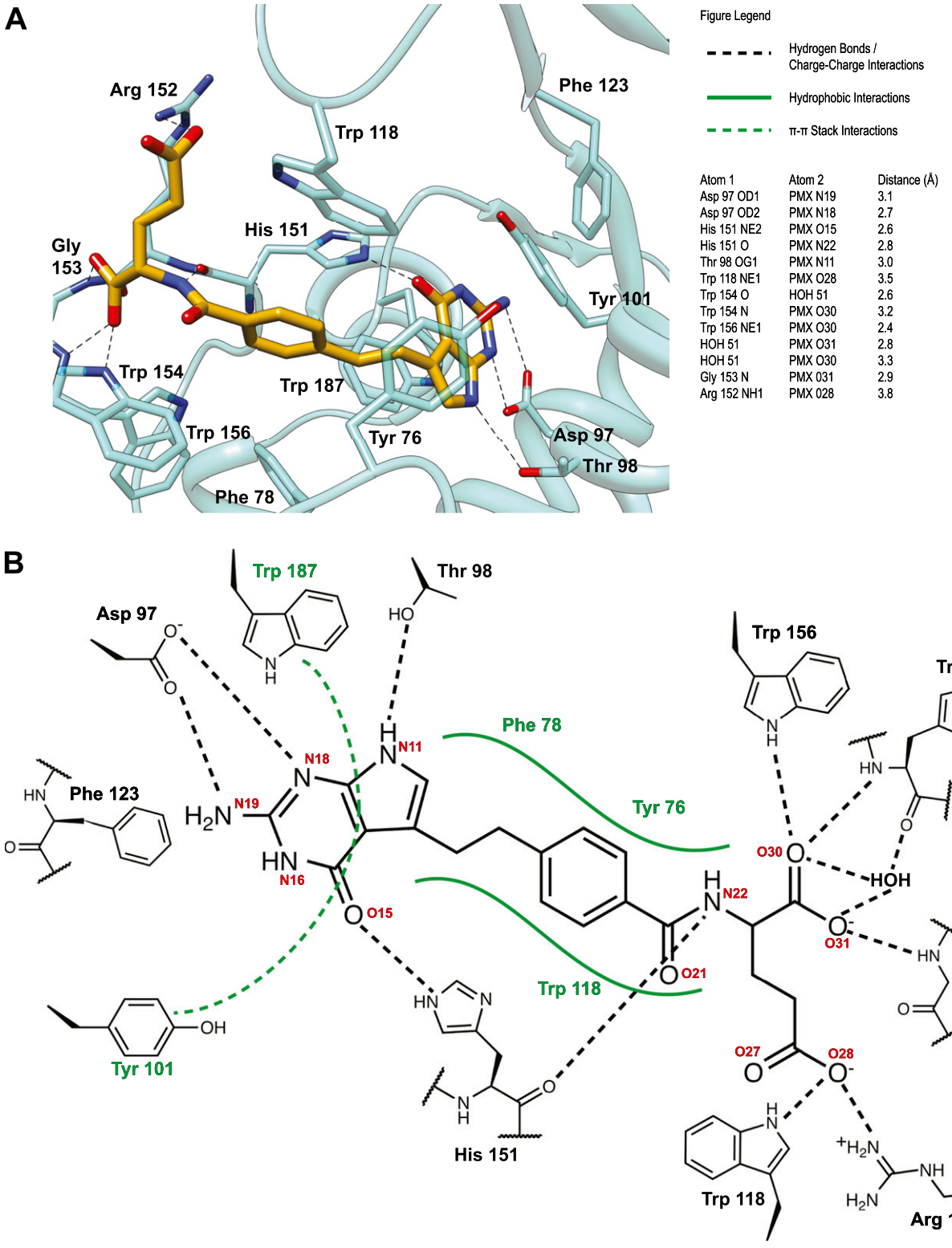

Fig. S4. Ligand interaction map of the hFRβ pemetrexed (PMX) complex structure. (*A*) The cartoon image highlights residues in the binding pocket that make direct contact with the antifolate PMX. (*B*) The ligand map shows a schematic of interacting residues. Contact types are listed in the legend in the upper right. Distances between atoms in polar contacts are listed in the table inset.

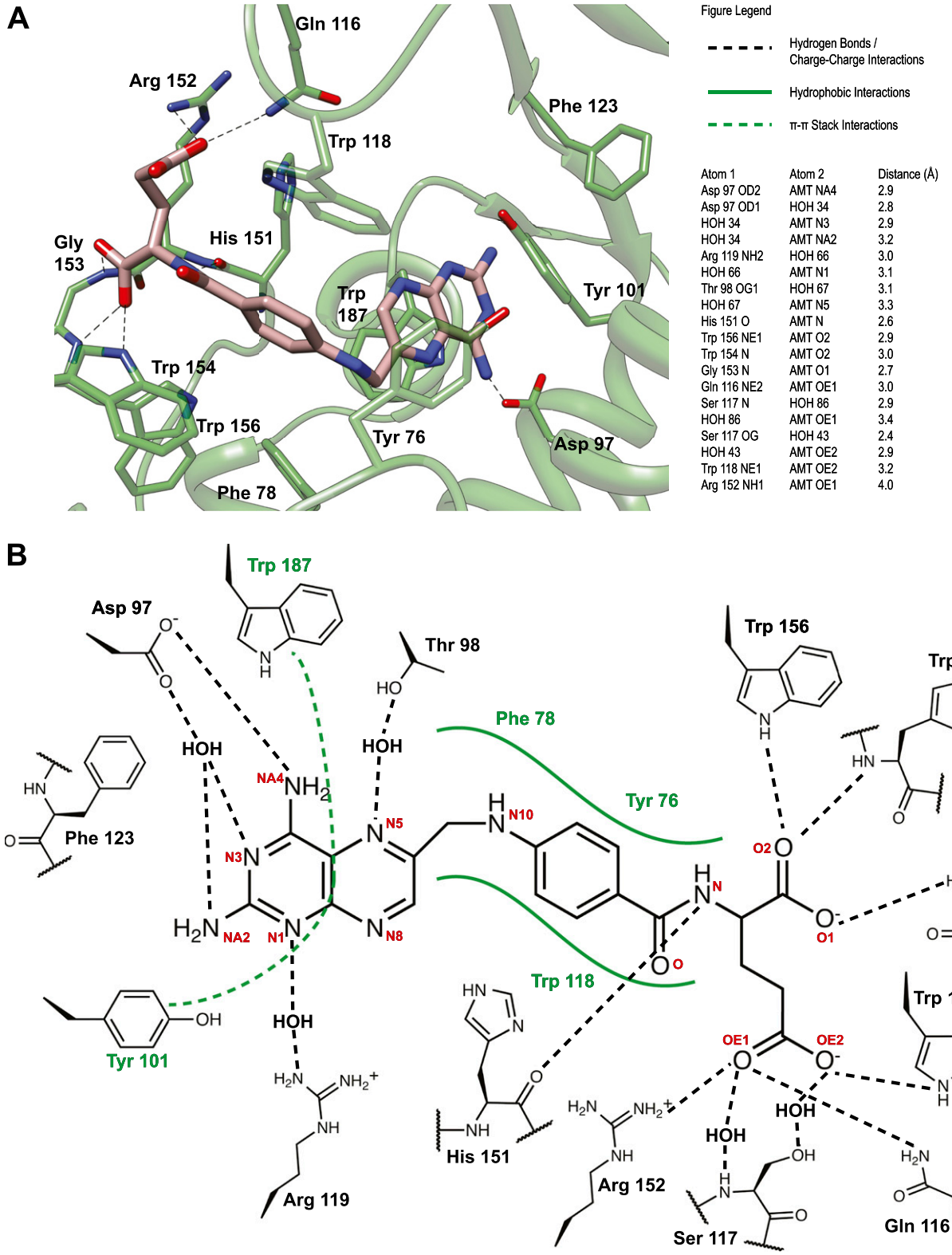

Fig. S5. Ligand interaction map of the hFRβ aminopterin (AMT) complex structure. (*A*) The cartoon image highlights residues in the binding pocket that make direct contact with the antifolate AMT. (*B*) The ligand map shows a schematic of interacting residues. Contact types are listed in the legend in the upper right. Distances between atoms in polar contacts are listed in the table inset.

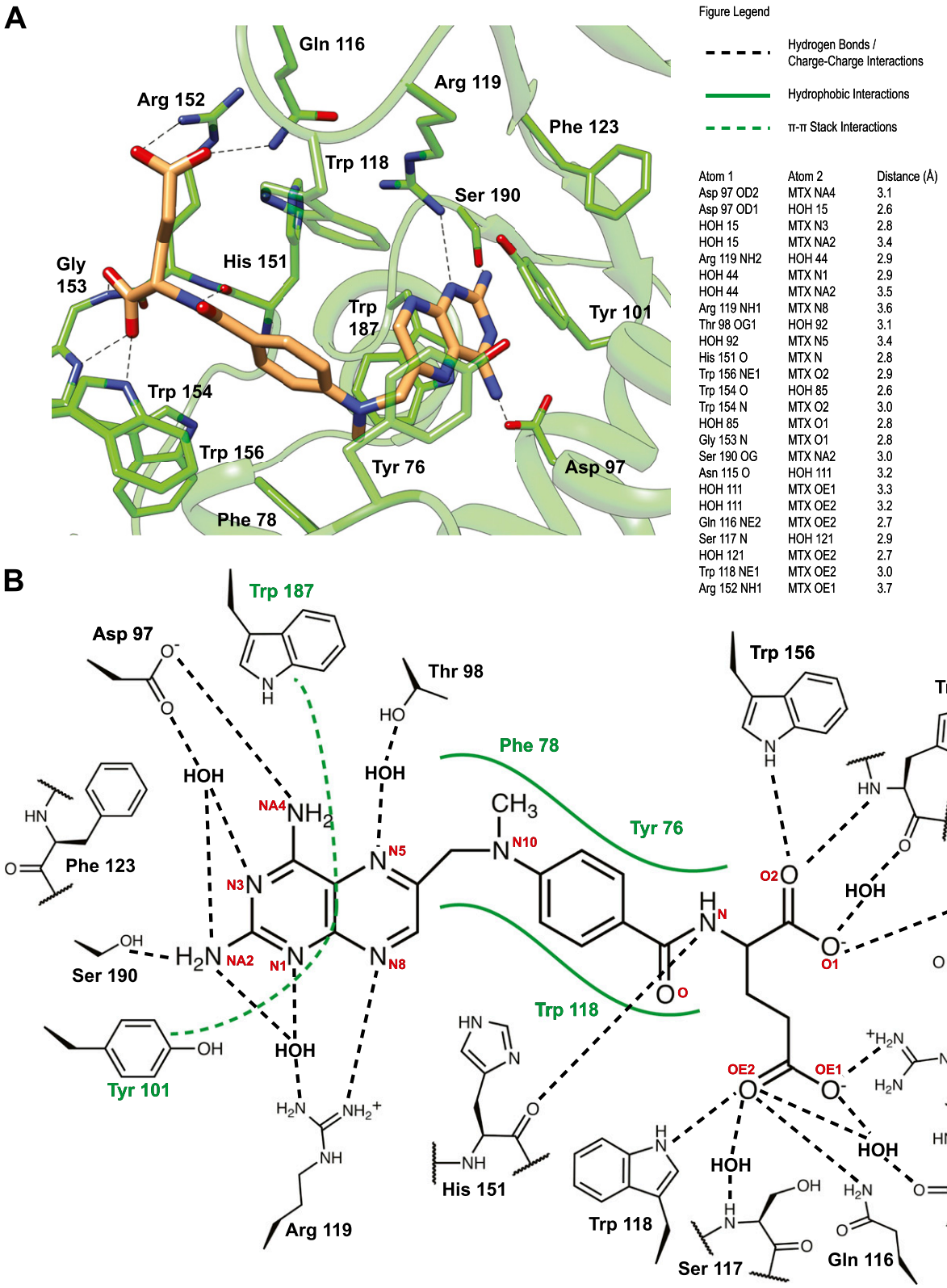

Atom 1	Atom 2	Distance (Å)
Asp 97 OD2	MTX NA4	3.1
Asp 97 OD1	HOH 15	2.6
HOH 15	MTX N3	2.8
HOH 15	MTX NA2	3.4
Arg 119 NH2	HOH 44	2.9
HOH 44	MTX N1	2.9
HOH 44	MTX NA2	3.5
Arg 119 NH1	MTX N8	3.6
Thr 98 OG1	HOH 92	3.1
HOH 92	MTX N5	3.4
His 151 O	MTX N	2.8
Trp 156 NE1	MTX O2	2.9
Trp 154 O	HOH 85	2.6
Trp 154 N	MTX O2	3.0
HOH 85	MTX O1	2.8
Gly 153 N	MTX O1	2.8
Ser 190 OG	MTX NA2	3.0
Asn 115 O	HOH 111	3.2
HOH 111	MTX OE1	3.3
HOH 111	MTX OE2	3.2
Gln 116 NE2	MTX OE2	2.7
Ser 117 N	HOH 121	2.9
HOH 121	MTX OE2	2.7
Trp 118 NE1	MTX OE2	3.0
Arg 152 NH1	MTX OE1	3.7

Fig. S6. Ligand interaction map of the hFRβ methotrexate (MTX) complex structure. (*A*) The cartoon image highlights residues in the binding pocket that make direct contact with the antifolate MTX. (*B*) The ligand map shows a schematic of interacting residues. Contact types are listed in the legend in the upper right. Distances between atoms in polar contacts are listed in the table inset.

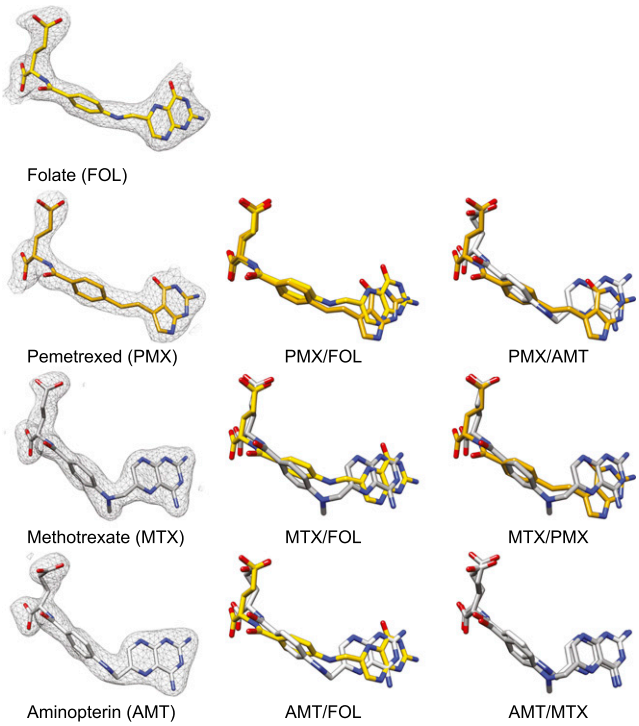

Fig. S7. Comparison of ligand binding modes in hFRβ complexes. Individual ligands are shown with final refined $2m|F_o\text{-}DF_c|$ electron density maps contoured at 1.0 σ. Folate binds similarly to all ligands at the gluatamyl tail, with variations in binding modes between ligands seen primarily in the aromatic systems that substitute for the pterin ring of folate. The pyrrolo-pyrimidine in PMX binds with the same ring orientation as folate, although clearly rotated, with the exocyclic oxygen making similar contacts in the binding pocket. In contrast, AMT and MTX bind with the diaminopteridine moiety rotated 180° (flipped) relative to the pterin of folate.

Table S1. X-ray crystallographic data for FR apo structures

	Apo hFRβ	Apo hFRα Kif-EndoH	Apo hFRα	Apo hFRα
PDB ID	4KMY	4KM6	4KMX	4KM7
Expression host	CHO	CHO	*Sf9*	*Sf9*
Crystallization pH*	**7.4**	**5.5**	**5.5**	**5.5**
Data collection				
Space group	$P6_1$	$P\ 2_1\ 2_1\ 2_1$	$P6_5$	P 1
Cell dimensions				
a, b, c (Å)	a = 75.16, c = 97.27	36.52, 63.34, 71.17	99.19, 99.19, 56.87	33.71, 55.38, 69.50
α, β, γ (Å)				72.23, 86.95, 90.12
Molecule per a.s.u	1	1	1	2
Resolution	50–1.80 (1.83–1.8)	50–1.55 (1.58–1.55)	30–2.20 (2.24–2.2)	50–1.80 (1.83–1.80)
I/σI	15.4 (2.3)	15.3 (2.7)	13.8 (1.6)	10.3 (7.2)
Completeness (%)	100.0 (99.8)	98.3 (86.8)	96.4 (90.4)	97.8 (99.1)
Redundancy	7.8 (4.6)	5.7 (4.5)	5.4 (3.2)	3.4 (3.4)
R_{sym}	10.0 (55.6)	8.7 (49.5)	9.6 (57.4)	10.0 (18.0)
	Apo hFRβ	Apo hFRα	Apo hFRα	Apo hFRα
Refinement				
Resolution (Å)	50–1.8 (1.83–1.8)	32.4–1.55 (1.58–1.55)	30–2.2 (2.26–2.2)	28.1–1.8 (1.84–1.8)
No. reflections				
Used for refinement	28,939	23,197	15,746	42,731
Used for R_{free} calculation	1,199	1,906	790	1,980
R_{factor} (%)	16.4 (21.2)	16.8 (23.2)	17.2 (24.5)	22.2 (22.4)
R_{free} (%)	19.3 (24.9)	19.9 (27.9)	19.9 (26.5)	26.9 (28.0)
No. atoms				
Protein	1,667	1,667	1,617	3,154
Ligand	NA	NA	NA	NA
Metals	1	1	2	2
Carbohydrates	14	42	24	56
Water molecules	164	127	162	440
B-factors (Å2, average)				
Protein	31.2	21.4	32.8	14.7
Ligand	NA	NA	NA	NA
Metals	26.7	16.4	30.9	13.5
Carbohydrates	39.1	39.4	57.2	33.2
Water molecules	40.9	28.5	39.5	26.6
r.m.s. deviations				
Bond lengths (Å)	0.009	0.007	0.004	0.006
Bond angles (°)	1.113	1.161	0.797	1.029

Values in parentheses are for the highest resolution shell. NA, not applicable.
*Reported pH is measured value for the mixture of final protein buffer and crystallant solution.

Table S2. X-ray crystallographic data for FR complex structures

	hFRβ/folate	hFRβ/methotrexate	hFRβ/aminopterin	hFRβ/pemetrexed
PDB ID	4KMZ	4KN0	4KN1	4KN2
Expression host	CHO	CHO	CHO	CHO
Crystallization pH*	8.0	8.0	8.0	8.2
Data collection				
Space group	$P6_122$	$P6_122$	$P6_122$	$I4_122$
Cell dimensions				
a, b, c (Å)	a = 96.86, c = 98.34	a = 97.60, c = 99.37	a = 97.08, c = 98.96	a = 97.44, c = 348.11
Molecule per a.s.u	1	1	1	3
Resolution	50–2.3 (2.34–2.3)	50–2.10 (2.14–2.1)	50–2.3 (2.34–2.3)	50–2.6 (2.64–2.6)
I/σI	22.0 (1.8)	16.8 (3.9)	12.4 (2.9)	16.2 (2.2)
Completeness (%)	95.2 (85.5)	100.0 (99.8)	98.4 (97.4)	100.0 (100.0)
Redundancy	11.1 (8.6)	8.7 (6.9)	10.6 (10.2)	8.1 (8.2)
R_{sym}	8.9 (48.9)	12.3 (49.5)	15.5 (59.8)	11.3 (67.5)
Refinement				
Resolution (Å)	48.4–2.3 (2.39–2.3)	42.8–2.1 (2.21–2.1)	50–2.3 (2.34–2.3)	50–2.6 (2.64–2.6)
No. reflections				
Used for refinement	12,030	16,841	12,543	26,486
Used for R_{free} calculation	1,203	987	1,002	1,341
R_{factor} (%)	20.5 (28.4)	17.8 (20.9)	18.8 (20.1)	19.4 (24.5)
R_{free} (%)	26.0 (36.4)	23.1 (26.8)	23.5 (25.8)	24.4 (30.2)
No. atoms				
Protein	1,630	1,641	1,656	4,821
Ligand	32	33	32	93
Metals	2	3	4	6
Carbohydrates	28	56	50	42
Water molecules	50	228	111	115
B-factors (Å2, average)				
Protein	42.4	23.2	34.9	47.6
Ligand	42.8	25.1	38.6	52.1
Metals	56.3	44.08	60.3	56.7
Carbohydrates	64.3	53.3	75.1	39.6
Water molecules	42.6	33	38.5	42.3
r.m.s. deviations				
Bond lengths (Å)	0.006	0.013	0.004	0.008
Bond angles (°)	0.93	1.266	0.823	1.067

Values in parentheses are for the highest resolution shell.
*Reported pH is measured value for the mixture of final protein buffer and crystallant solution.

Table S3. Thermodynamic analysis of folate and antifolate binding to FRs

Ligand	pH	K_d (nM)	ΔG (kcal/mol)	ΔH (kcal/mol)	$-T\Delta S$ (kcal/mol)
hFRα thermodynamic binding parameters					
Folic acid	7.4	0.0103 ± 0.0015	−15.0 ± 0.1	−27.7 ± 0.1	12.7 ± 0.1
	6.5	21 ± 9	−10.5 ± 0.3	−25.2 ± 1.2	14.7 ± 1.4
Methotrexate	7.4	65 ± 5	−9.7 ± 0.3	−17.8 ± 0.5	8.1 ± 0.2
	6.5	88 ± 5	−9.6 ± 0.1	−17.4 ± 0.6	7.8 ± 0.6
Aminopterin	7.4	65 ± 6	−9.8 ± 0.1	−18.1 ± 1.1	8.3 ± 1.0
	6.5	71 ± 7	−9.8 ± 0.1	−16.8 ± 0.9	7.1 ± 0.9
Pemetrexed	7.4	4.5 ± 1.9	−11.4 ± 0.3	−20.1 ± 0.7	8.7 ± 0.9
	6.5	11 ± 2.5	−10.9 ± 0.1	−27.6 ± 0.2	16.7 ± 0.3
hFRβ thermodynamic binding parameters					
Folic acid	7.4	2.7 ± 1.5	−11.8 ± 0.4	−26.3 ± 0.7	14.5 ± 0.9
	6.5	23 ± 5	−10.4 ± 0.1	−10.3 ± 0.2	−0.1 ± 0.2
Methotrexate	7.4	40 ± 7	−10.1 ± 0.1	−16.4 ± 0.2	6.3 ± 0.3
	6.5	332 ± 64	−8.8 ± 0.1	−6.2 ± 0.1	−2.6 ± 0.2
Aminopterin	7.4	144 ± 5*	−9.3 ± 0.1	−10.7 ± 0.5	1.4 ± 0.6
	6.5	ND	ND	ND	ND
Pemetrexed	7.4	54 ± 17	−9.9 ± 0.2	−8.0 ± 0.3	−1.9 ± 0.5
	6.5	323†	−8.9	−5.9	−3.0

Unless noted, all measurements include SD from at least four trials. ND, not determined.
*Two measurements.
†Single measurement.

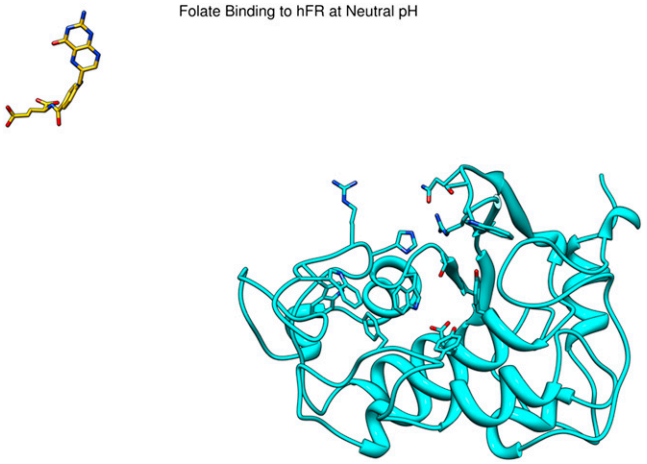

Movie S1. Transition from state I (apo) to state II (folate complex) of the hFR showing movement of residues that interact with folate.

Movie S1

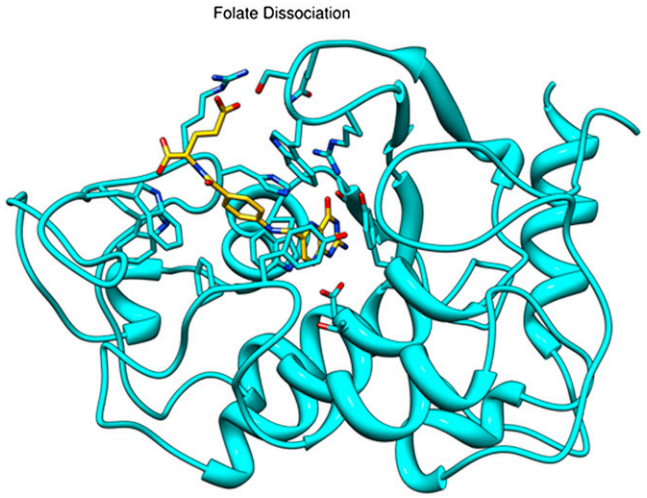

Movie S2. Transition from state II (folate complex) to state III (acidic) of the hFR showing movement of residues that interact with folate.

Movie S2

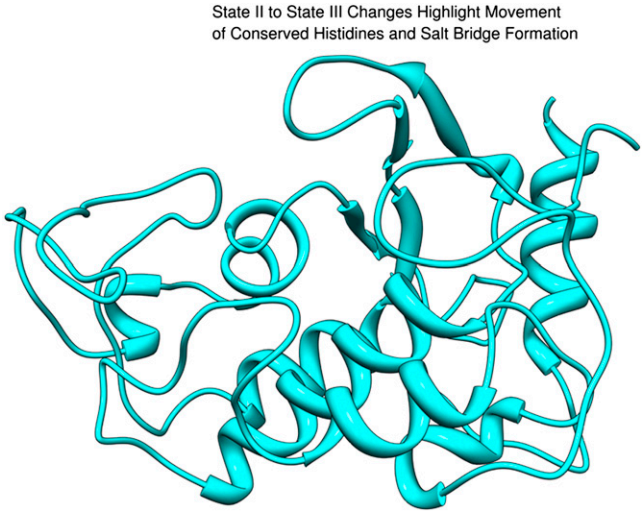

Movie S3. Transition from state II (folate complex) to state III (acidic) of the hFR showing movement of histidines and ionic interactions with R125.

Movie S3